HardwareX 10 (2021) e00218

Contents lists available at ScienceDirect

HardwareX

journal homepage: www.elsevier.com/locate/ohx

Automated low-cost device to produce sub-micrometric polymer fibers based on blow spun method

José E. Domínguez [a,b,*], E Olivos [b], Carlos Vázquez [c], J.M. Rivera [d], Rigoberto Hernández-Cortes [e], Javier González-Benito [a]

[a] Department of Materials Science and Engineering and Chemical Engineering, IQMAAB, Universidad Carlos III de Madrid, Madrid, Spain
[b] Department of Nanotechnology, INTESU, Universidad Tecnológica del Centro de Veracruz, Mexico
[c] Institute of Industrial Engineering and Automotive Mechanics, Universidad Tecnológica de la Mixteca, Mexico
[d] LADISER Organic Chemistry, Faculty of Chemical Sciences, Universidad Veracruzana, Orizaba, Mexico
[e] Department of Economics and Management, Universidad Veracruzana, Orizaba, Mexico

ARTICLE INFO

Article history:
Received 17 May 2021
Received in revised form 11 July 2021
Accepted 28 July 2021

Keywords:
Solution Blow Spinning (SBS)
Polysulfone Fibers
Collector Influence

ABSTRACT

Attending the latest advances in polymeric fibers, the design of low-cost, and high-quality scientific equipment for obtaining fibers seemed essential. To overcome this challenge, a 3D printable prototype was designed, assembled, and validated to obtain fibers using the SBS method. The particular configuration of the prototype consisted of controlling the process conditions such as working distance and injection flow, as well as other parameters such as RPM and the axial movement of the cylindrical collector. Thus, these parameters were automated using a microcontroller (Arduino) that receives information from an Android device with bluetooth connectivity to control each of the elements of the equipment. Subsequently, the repeatability and reproducibility of the fibers was verified using polymers such as polystyrene (PS), polysulfone (PSF) and polyethylene oxide (PEO); furthermore, PSF fibers were manufactured to analyze the influence of working distance and the axial movement of the collector on their production.

Hardware name	Automated low-cost device to produce sub-micrometric polymer fibers based on SBS method
Subject area	• Engineering and Material Science • General
Hardware type	• Mechanical engineering and materials science • Other. - Synthesis of materials
Open Source License	CC BY 4.0
Cost of Hardware	$245.93
Source File Repository	https://doi.org/10.17632/spccrzhtyh.1

* Corresponding author at: Universidad Tecnológica del Centro de Veracruz. Avenida Universidad 350, 94910 Cuitláhuac, Veracruz. Mexico.
E-mail address: jose.dominguez@utcv.edu.mx (J.E. Domínguez).

https://doi.org/10.1016/j.ohx.2021.e00218
2468-0672/

Hardware in context

Micro and nanofibers have been widely used for different applications such as drug delivery, water filtration, energy storage, protective clothing, among others due to their excellent properties. Nevertheless, commercial devices to produces them are expensive.

3D printed devices have had great technological advances and a significant reduction of costs in recent years. Furthermore, easy accessibility to open-source hardware's has allowed the rapid manufacture of replicated prototype [1,2] without expensive industrial infrastructure [3] and excessively high return on investment [4].

The design of open hardware prototypes has facilitated the construction of low-cost laboratory devices or tools as a rotary sample mixer-agitator [5], nutate mixer [6], syringe pump [7,8], injectors adapters [2,9], among others. In addition, complete instrument to measure has been created by open source hardware as optical equipment's [10], light microscope control and optical projection tomography (OPT) configurations [11], mechanical opto-cage system with enclosure [12], pH meter [13], and others. The construction of open-source hardware allows to manufacture low-cost devices for different areas of knowledge.

Nowadays, electrospinning is one of the most suitable method for producing continuous nanomaterials with varying physical, chemical and biological properties [14]. However, the disadvantage of this technique is the high energy consumption required to produce, difficult to make a large volume scafford [15] and the cost of commercial equipment. To reduce the cost of commercial equipment, it has been presented the development of an electrospinning-based rapid prototyping (ESRP) technique for the fabrication of patterned scaffolds from fine fiber with high repeatability and reproducibility [16]. However, Solution blow spinning (SBS) is a maturing and facile nanofiber fabrication technology, this method produces fibers from a polymer dissolution through the use of pressurized gas. It has high yield, short preparation time and high usage value besides, it requires a relatively wide polymer dissolution, and the spinning solution is relatively wide [17]. SBS is based on the use of a concentric nozzle in which the inner channel extrude a polymer dissolution while along the outer one pressurized gas is passed to push the polymer dissolution at the nozzle exit forming fibers that finally are deposited in a collector or substrate located at a particular working distance [18], so nozzle is the principal component of SBS, there are some home-made nozzles to produce fibers with SBS technology, however, there are not information enough about the way to create them. In this sense, it would be important to describe in detail the way to create a nozzle to produce fibers using a 3d printer. Besides, it would be also important to automate the processing conditions through the control of the corresponding parameters ensuring repeatability of manufactured materials.

Hardware description

The device was designed by modularity concept, because by user modularity updating, devices improve versatility in terms of modifying the production parameters. The device was divided in three modules, the first one allows producing fibers by controlling the injection rate and rotational speed (RPM) of the collector. The second module controls motion of the collector along the "y" axis and the third module controls the working distances between nozzle and the collector.

Module one

Module one is constituted by the syringe pump and the collector, both controlled by the Arduino, and a 3D printed nozzle. The syringe pump is based on a stepper motor that rotates a threaded rod to push a block that press the Syringe plunger. Syringe pump component is formed by 2 printable parts (002 Mod2 and 003 Mod2) in order to decrease the number printable parts compared to others more conventional; besides, it uses just one guide for the pusher block [7,8,19]. Collector is formed by a DC motor, collector holder (004 Mod1) and container with lid. RPM of collector and the weight of the container is limited by the specifications of the DC motor. Collection of fibers dependents on the surface area of the container used and the displacement along the "Y" axis of the collector (Module 2).

The nozzle is the main component of the device since this component is responsible of fibers production at the micro and nano scale. Different home-made nozzles can be found in the literature [18,20–22], however they are made by manufacturing processes or assembling several parts. The drawback of these home-made and commercial nozzles basically lies on the difficulty of their modifications to control processing conditions through several parameters such as nozzle diameter or nozzle geometry. Besides, home-made nozzles usually do not ensure inner and outer nozzle to be completely concentric.

Fig. 1 shows a lateral cross-section view of nozzle, it is formed by three parts: needle, pneumatic connector, and printable nozzle. Pneumatic connector fits the tubing that transport the pressured gas, Needle transports the polymer disolution injected by the syringe pump and, printable nozzle guides the pressured gas to stretch the polymer disolution. Printable nozzle design could be modified to change the geometry of the outer nozzle in order to modify its diameter and therefore be able to host needles with different diameters.

Polymer dissolution is injected in inner nozzle at a controlled flow rate while along the outer nozzle is inserted the air to finally eject the dissolution towards the collector.

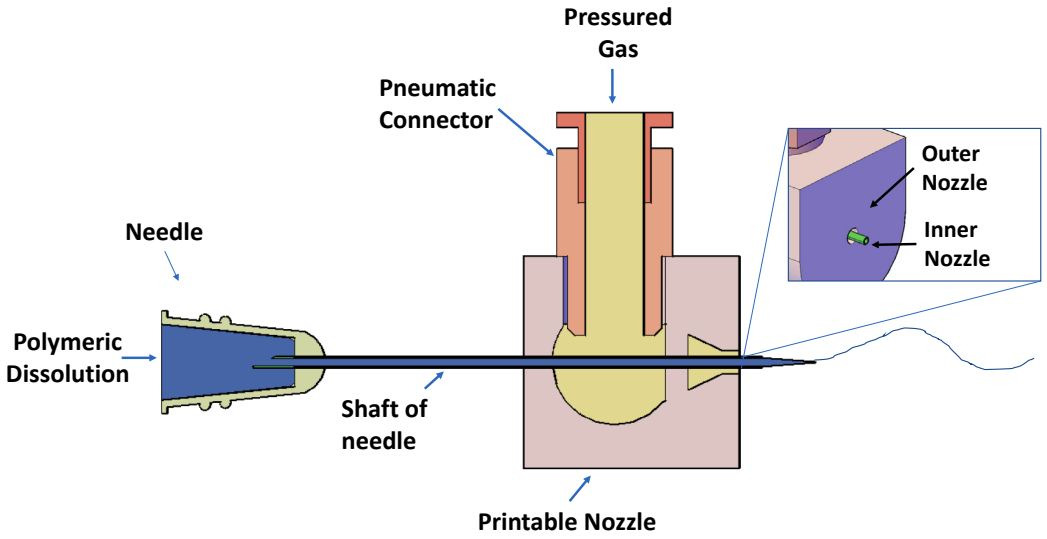

Fig. 1. Lateral view of nozzle.

Module two

The second module (Fig. 2) allows collector displacement along the "y" axis. It is noteworthy here that the collector motion is preferred to the nozzle displacement, due to vibration accumulation of dissolution at the needle tip of the nozzle can occur hindering fiber formation [16].

The axial movement is based on a belt and pulley driven linear motion system operated by Arduino controller. The axial movement of the cylindrical collector has not been registered yet for solution blow spinning technique. It was studied for electrospinning, but almost all references are more focused on controlling the homogeneity of material collected by the applied electric field [23,24]. In the SBS, there is not any evidence of controlling homogeneity of the materials produced.

Module three

Although working distances has spinnability influence [25,26], it has little effect on diameter of fibers [27,28]. Thus, the optimum choice of working distances is an important factor to take into account from lab-scale to manufactory industry. Short working distances could result in semi-solidified fibrous structure while for large distances solvent would have more

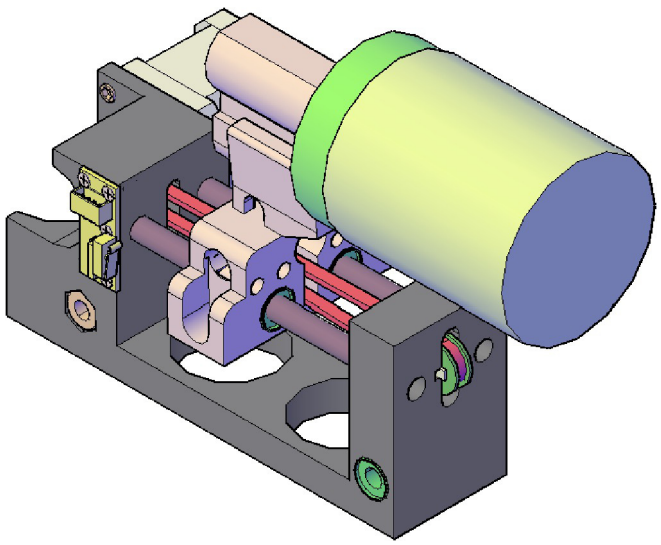

Fig. 2. Module 2 or component to move the collector.

time for the evaporation and therefore beaded free fibers would be collected [25,27]. On the other hand, as working distance increases, the formed fibers have more probability of flying away far from the collector leading to reduction of fiber collection. So, controlling working distance might have great effect on the material production by SBS.

The axial movement mechanism, module 3 (Fig. 3) is entirely made with stainless-steel threaded rod and hexagonal nuts inserted in the base of the Axis "y" body (005 Mod2). Linear bearings were used to guide the base of axis "y".

Design files

All the components were designed in Autodesk (Free students and educators version), then the designs were exported to Surface Tessellation Language format (*.stl). To transmit the three dimensions surface geometry, the STL files were processed with CURA software to obtain the G codes used by the 3D printer to manufacture each piece.

3D printer with Fused Deposition Modeling technology (FDM) brand Comgrow Creality Ender 3 was used. Polylactic acid filament (PLA) was extruded using 0.4 mm diameter nozzle, 200 °C, layer height of 0.3 mm and 30% of fill. Due to versatility of PLA, modern industrial uses, and performance to be printable, PLA was used as testing material. The PLA nozzle exhibited no evidence of wear as long as the dissolution did not make contact with it. It is recommended to look for another material for industrial scalability purposes.

Summary of the files required to produce the open-source device are available in the Table 1.

The repository project includes the source code for IDE Arduino software, 3d printed components in STL format for 3D printer Ender 3 and, original CAD models created with the software AutoCAD (student version).

The description of the files is listed below:

001 Mod1: The nozzle is the main component of the open-source device, it allows to flow the air by 3D printable component and the polymeric dissolution by the needle holder.

002 Mod2: Injection Pump body; this contains itself the syringe holder block and motor holder block.

003 Mod3: Pusher block; it captures the syringe's plunger flange. It is driven by the lead screw and is supported by the guide rods and lead screw.

004 Mod1: Collector holder; it supports the container used as collector.

005 Mod2: Axis "y" body; this component holds mechanical elements to move the collector in axis "y".

006 Mod2: Support block axis "y"; this element holds the DC motor support and is moved by belt connected to step motor.

007 Mod2: DC motor support; this element is designed to be modified according the DC motor dimensions.

008 Mod2: Belt pulley; this component is attached in step motor shaft and moves the belt of axis "y".

009 Mod2: Idler pulley; it is responsible for guiding and the engine drive belt.

010 Mod2: Idler pulley limit; it works to limit the linear pulley to a specific space in the Axis "y" body

011 Mod3: Holder axis "x"; step motor and nozzle are supported in this component.

012 Mod3: Guide axis "x"; guide rod of axis "X" is supported in this element.

Electronic design

In order to use of device separately (module by module), the electronic circuits were separated in three parts. The first one controls the syringe pump and the speed of collector, the second govern the movement of the collector along the axis "y" and the last one controls the work distance between the nozzle and the collector.

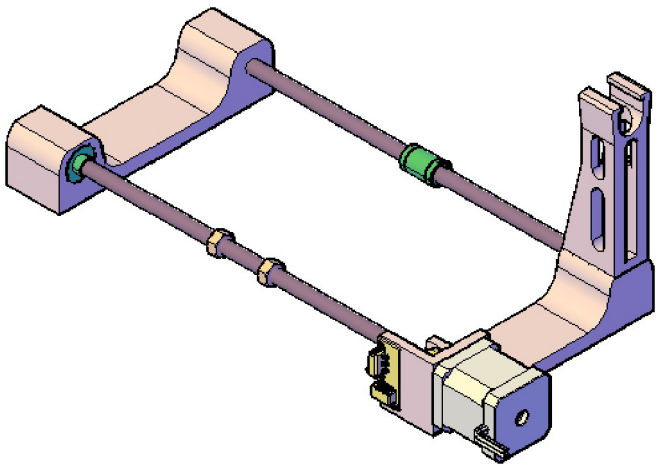

Fig. 3. Component to control the working distance.

Table 1
Design Files Summary.

Design file name	File type	Open Source license
001 Mod1	CAD file & STL file	CC BY 4.0
002 Mod1	CAD file & STL file	CC BY 4.0
003 Mod1	CAD file & STL file	CC BY 4.0
004 Mod1	CAD file & STL file	CC BY 4.0
005 Mod2	CAD file & STL file	CC BY 4.0
006 Mod2	CAD file & STL file	CC BY 4.0
007 Mod2	CAD file & STL file	CC BY 4.0
008 Mod2	CAD file & STL file	CC BY 4.0
009 Mod2	CAD file & STL file	CC BY 4.0
010 Mod2	CAD file & STL file	CC BY 4.0
011 Mod3	CAD file & STL file	CC BY 4.0
012 Mod3	CAD file & STL file	CC BY 4.0

The schematic diagram for the electronic circuitry of modules is shown in Fig. 4. The modules are basically made up of Arduino Nano microcontrollers, A9488 stepper driver, NEMA 17 stepper motor, DC motor, TB6612FNG DC motor driver, bluetooth module, switch, and career switch. Power inputs for motors were 12 V and microcontroller and driver were 5 V.

The wires were classified according to function, black wire is used to GND connection, 5 V is identified to orange wire while 12 V to red wire. Green wires identify inputs and outputs between components.

Bill of materials

Bill of materials (Table 2) shows the generic name of the component, code component given by supplier, number of components, individual cost, and total cost. Total bill of material necessary to assemble the components was 234.77 dollars. In the same way, considering an average price of PLA (1 kg), 3D print cost was obtained to 11.21 dollars (Table 3).

Bill of Materials and printable components cost are $245.93, compared with commercial and homemade system, the cost was cheap.

Build instructions

The device assemble was divided in 3 modules, the first one shows the simplest way to produce fibers without automated system. Then, assemble of collector with automated movement of axis to create a homogenous surface in the whole collector and the last one is the assemble of automated work distance.

Nozzle assembly

The nozzle assemble (Fig. 5) can be described as follows:

1. Pint “001 Mod1” file (Nozzle).
2. Use the die set to create the internal thread in the nozzle (1) and screw in the pneumatic connector (2).
3. Use a drill to adjust the hole of the capillary bevel and insert the needle (3) (nozzle was designed s default to G14 needle).

Syringe pump assembly

The syringe pump assemble (Fig. 6) can be described as follows:

1. Pint “002 Mod1” (syringe pump body) and “003 Mod1” (pusher block).
2. Anchor NEMA motor (1) in the motor holder in the syringe pump body (2) and fix with screws (3).
3. Snap on the linear ball bearing (4) at the bottom of the pusher block (5).
4. Slice a length of 15 cm of Steel Linear Shaft Axis (6) and slide it through the bottom of the syringe pump body (2) and the linear bearing inserted in the pusher block (5)
5. Attach the flexible shaft coupling (7) in step motor shaft (1) and secure in it.
6. Slice a length of 12.5 cm of Stainless-steel threaded rod (8) and slide it in the top of syringe pump body (2) while screw it in the pusher block (5) and secure the stainless-steel with the flexible shaft coupling (7).
7. Snap on the Radial Ball Bearing (10) on the top of syringe pump body (2) and attach it.
8. locate the Career Switch (11) in its position on syringe pump body (2) and screw it with the M3 flat Head Screws (12).

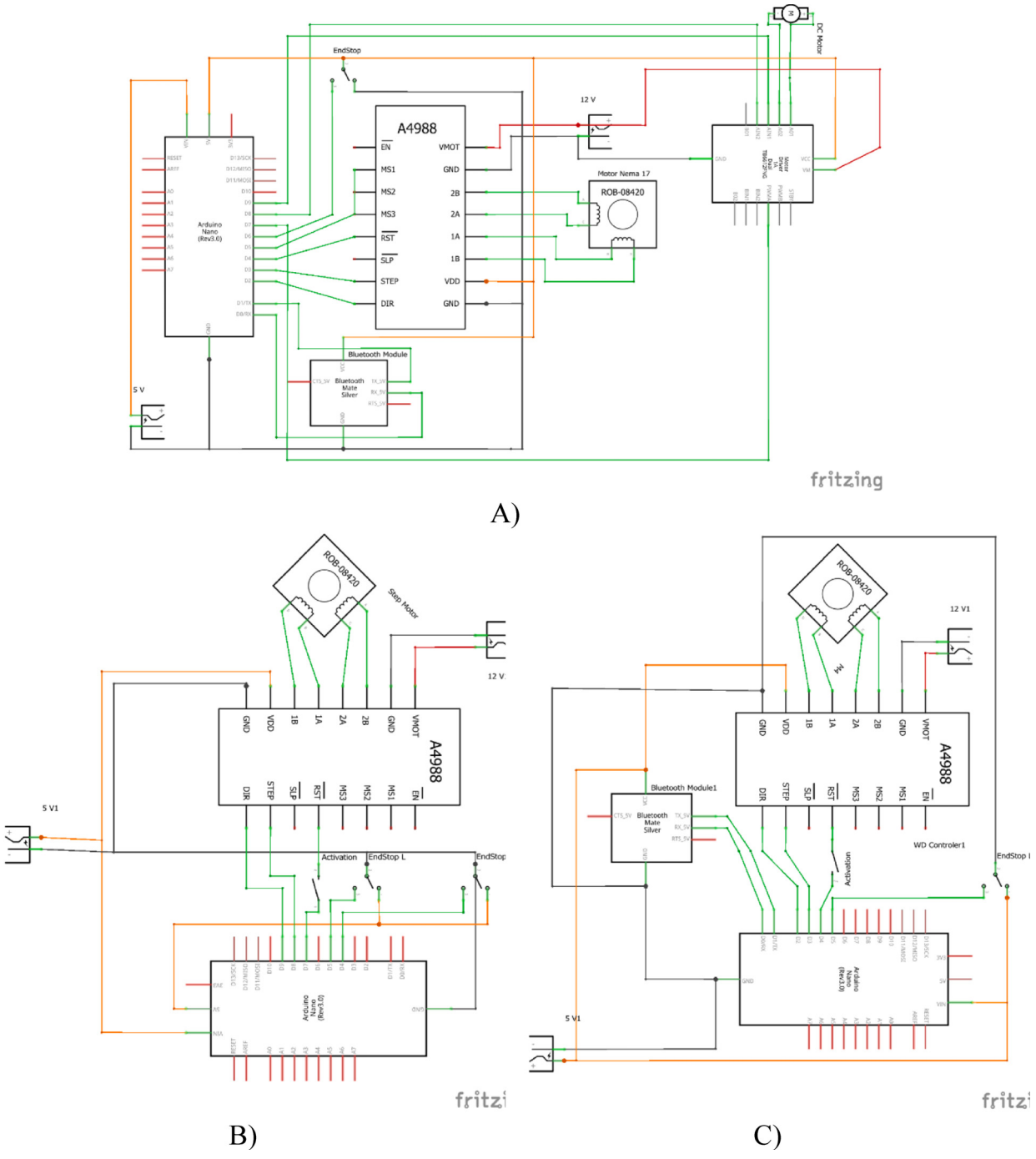

Fig. 4. Schematics circuits of module 1 (A), module 2 (B), and module 3 (C).

Collectors assembly

The collector assemble (Fig. 7) can be described as follows:

1. Print the collector holder (004 Mod1).
2. Drill four holes in the container lid (1) that fits with collector holder (2). Make sure that the concentric point of the holes fits with the Centre of the circumference of the container lid.
3. Fix the container lid (1) and collector holder (2) using the screws (3). it's possible use nuts to help the screws to hold correctly.

Table 2
Bill of Materials.

Designator	Component	Seller	Number	Material type	Cost per unit -currency	Total cost -currency
Arduino Nano	B0716T2L77	Amazon	3	Electronic	4.33	12.99
Driver 4988	B06ZZH81WT	Amazon	3	Electronic	1.99	5.97
Bluetooth module HC-05	B01G9KSAF6	Amazon	2	Electronic	9.99	19.98
Power Supply	B0788VTP9S	Amazon	3	Electronic	13.00	39.00
Career Switch	B06XS7FVTZ	Amazon	4	Electronic	2.20	8.80
Nema 17 Motor	B06XRFCP3X	Amazon	3	Electronic	13.00	39.00
DC Speed Reduction Motor	B07559RTFG	Amazon	1	Electronic	11.49	11.49
Motor Driver TB6612FNG	B078S6CWD2	Amazon	1	Electronic	19.61	19.61
Electronic board	B07Z61XPG9	Amazon	2	Electronic	2.00	4.00
wire	B01EV70C78	Amazon	1	Metal	6.81	6.81
Stainless steel threaded rod	10,282,601	Bricomart	1	Metal	3.43	3.43
flexible shaft coupling	YPN0037	Amazon	2	Metal	2.00	4.00
Blunt Tip Needles	B07JJ674NL	Amazon	1	Metal	14.98	14.98
Pneumatic Connector	B01EZZRWM4	Amazon	1	Polymer	0.86	0.86
Linear ball bearing	B06XGQSTTX	Amazon	5	Metal	0.92	4.60
Radial Ball Bearing	B01BH8EFZY	Amazon	2	Metal	2.68	5.36
Steel Linear Shaft Optical Axis	B01DXBG0HY	Amazon	4	Metal	4.39	17.56
Timing belt	B0768YSR82	Amazon	1	Polymer	12.99	12.99
Hexagonal nut 8 mm	90592A085	McMaster-Carr	3	Metal	0.30	0.90
Timing belts Tensioner Torsion spring	B076Q5WHSX	Amazon	2	Metal	0.30	0.60
M3 flat Head Screws	91290A115	McMaster-Carr	12	Metal	0.07	1.12
M3 Hexagonal nut	90591A121	McMaster-Carr	4	Metal	0.02	0.08
Rod	B083DY4FLN	Amazon	1	Metal	0.59	0.59
TOTAL	234.72					

Table 3
Bill of Printable components.

No.	Printable	3-D Printing Material	Quantity	Distance (m)	Mass (g)	Cost ($)
1	001 Mod1	PLA	1	1.36	4	0.1
2	002 Mod1	PLA	1	26.25	78	1.95
3	003 Mod1	PLA	1	5.21	16	0.4
4	004 Mod1	PLA	1	1.74	5	0.125
5	005 Mod2	PLA	1	38.01	113	2.825
6	006 Mod2	PLA	1	13.27	40	1
7	007 Mod2	PLA	1	7.46	22	0.55
8	008 Mod2	PLA	1	0.2	1	0.025
9	009 Mod2	PLA	1	0.52	2	0.05
10	010 Mod2	PLA	2	0.05	0.5	0.0125
11	011 Mod3	PLA	1	32.47	97	2.425
12	012 Mod3	PLA	1	23.58	70	1.75
TOTAL			13	150.12	448.5	11.21

4. Snap on the collector holder (2) the DC motor axis (4) and paste it with permanent glue. Be carefully don't paste the axis motor with the glue.
5. Screw the container (5) with the lid (1)

Axis "y" assembly (movement of collector)

The axis "y" assemble (Fig. 8) can be described as follows:

1. Print Axis "y" body (005 Mod2), Support block axis "y" (006 Mod2), DC motor support (007 Mod2), Belt pulley (008 Mod2), Idler pulley (009 Mod2), and Idler pulley limit (010 Mod2).
2. Snap on the linear ball bearing (1B) at the bottom of the support block axis (2B).
3. Fit pre-assembled collector DC motor (4B) on DC motor support (3B).
4. Slice a length of 13 mm of rod (3A), line up idler pulley (1A) and idler pulley limits (2A) and slide the rod (3A) through them to assemble the pulley block.
5. Hold the belt pulley (2) in step motor shaft (1).
6. Anchor Step motor (1) on axis "y" body (3) and fix it with the screws (4).

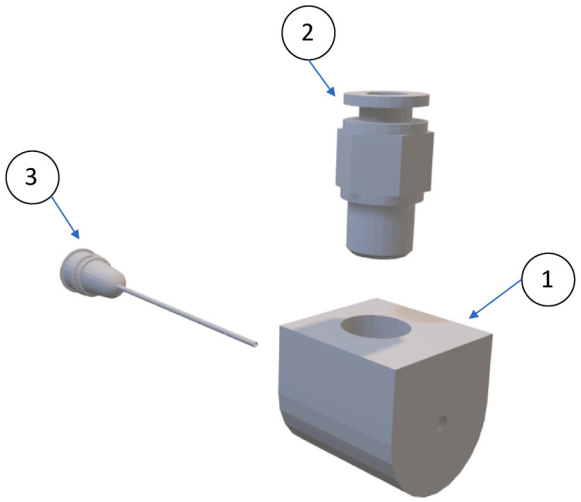

Fig. 5. Nozzle assembly.

7. Slice in duplicate a length of 12.5 cm of Steel Linear Shaft Axis (5) and slide them through the bottom axis "y" body (3) and the linear bearing inserted in support block axis (2B).
8. Place the Pulley block (6) on axis "y" body (3) and loop around the belt pulley (2) and pulley block (6) the timing belt and fastened with holders (1C).
9. Position the Career Switches (11) on axis "y" body (3) and screw them with the M3 flat Head Screws (8).
10. Slide the DC motor support (3B) on support block axis (2B).

Axis "x" assembly (Work distance controller)

The Axis "x" assemble (Fig. 9) can be described as follows:

1. Holder axis "x" (011 Mod3) and Guide axis "x" (012 Mod3) files should be printed.
2. Attach the flexible shaft coupling (2) in step motor shaft (1) and secure in it.
3. Anchor step motor (1) in the motor holder axis "x"(4) and fix with screws (3).
4. locate the Career Switch (5) in its position holder axis "x" (4) and screw it with the M3 flat Head Screws (6).
5. Slide linear bearings (1A) and snap on the hexagonal nuts (2A) in axis "y" pre-ensemble.
6. Slice a length of at least 30 cm of Steel Linear Shaft Axis (7) and slide it through motor holder axis "x" (4), linear bearing inserted in axis "y" pre-assemble and guide axis "x" (9).

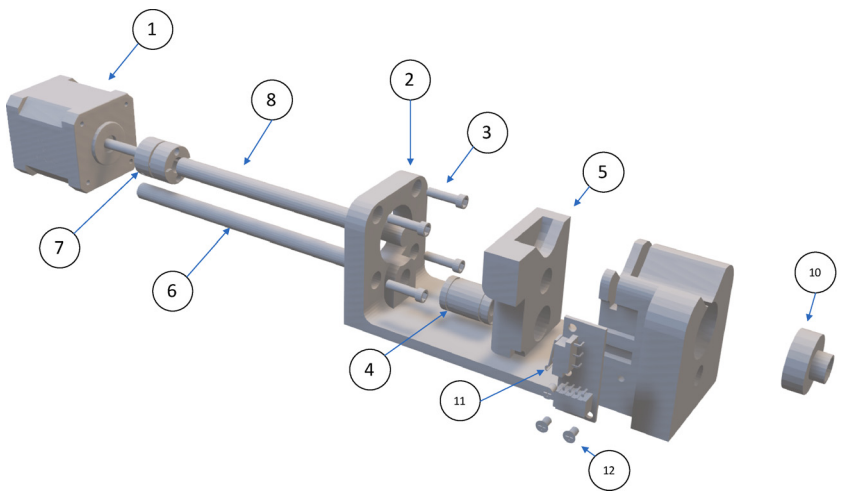

Fig. 6. Syringe pump assembly.

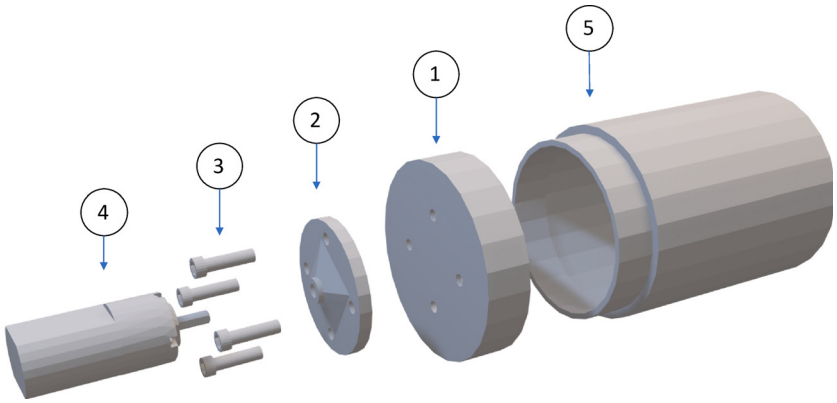

Fig. 7. Collector assemble.

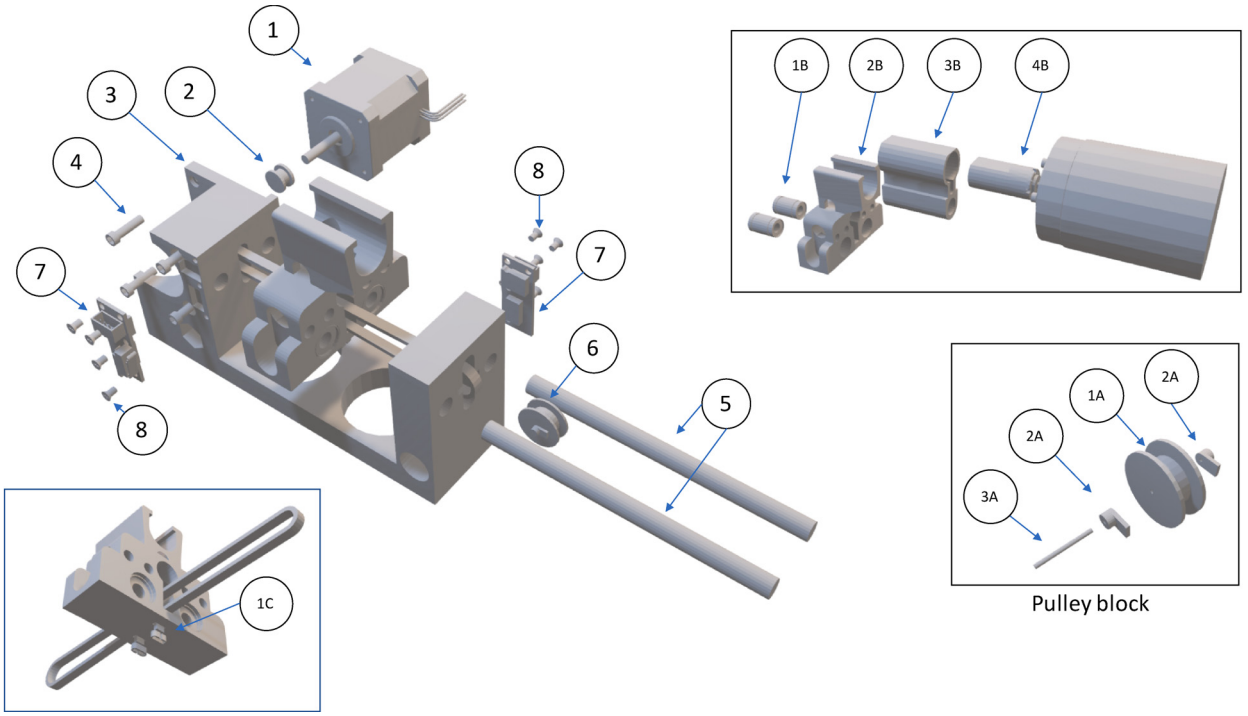

Fig. 8. Axis "y" assembly.

7. Snap on the radial Ball Bearing (10) on guide axis "x" (9).
8. Slice a length of at least 30 cm of Stainless-steel threaded rod (8), slide it through guide axis "x" (9), screw it through hexagonal nuts inserted in axis "y" pre-assemble and secure it on the flexible shaft coupling (2).

Electronic assembly

In this work, the electronic components such as Arduino, A4988 driver and others, were assembleon an electronic board using wire connections as it is shown in Fig. 10. Color code was used to identify each connection, red and orange wire were used for 12 V and 5 V voltage respectively while black wire corresponds to the ground, GND. Green color were used to differentiate between communication connectors.

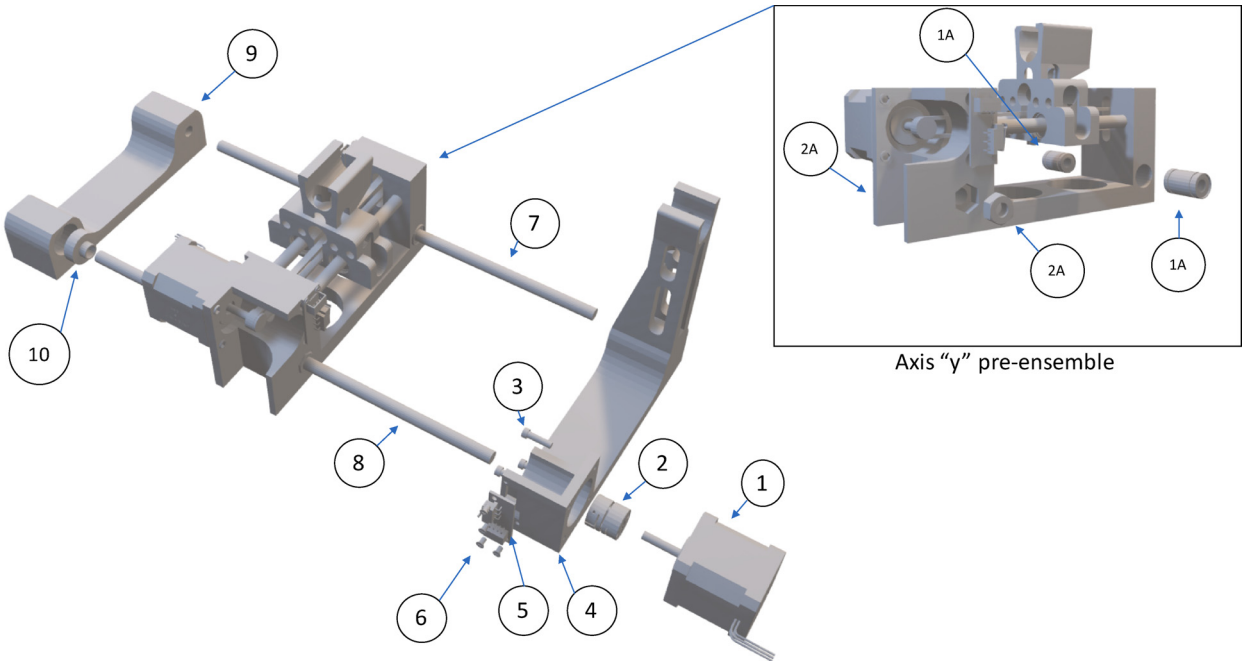

Fig. 9. Axis "x" assembly.

Operation instructions

Previous set up

After the complete assembly of components and connection of wires, the automated system should look as that one represented by the scheme shown in Fig. 11. Before produce fibers its necessary prepare the device. Firstly, air supply hose and nozzle assemble should be connected as indicate in Fig. 8A and B respectively; Second, use a 10 ml syringe to subtract the polymer dissolution and fit it on syringe pump (Fig. 8C); third turn on the power supply of device; and finally, open the air supply controlling the air flow with pressure gage according to experimental condition.

After preparing the device, it is necessary install in the android device an application to communicate the SBS system though the serial port of Arduino by bluetooth (BT). In particular, the free App "Arduino bluetooth controller" was selected and installed under android OS Version 10.1.

Production of fibers

Start the Arduino bluetooth controller and connect by BT with the BT name assigned for each component. After successful connection select "terminal mode" and a list of options will be displayed on the screen.

In the case of the first module, the displayed list asked for the rotation speed of collector in RPM (Fig. 12A), in this specific work, maximum speed of DC motor was 1000 RPM with 12 V taking it as the maximum speed (RPM depends on DC motor used and should be reprogrammed according to each DC motor). After selecting the rotational speed of the collector, a second list of commands appears asking for the flow rate of syringe pump (Fig. 12B). For the second module, working distance and movement of the collector are programmed in the same list (Fig. 12C), with number 1 or 2 it is possible to increase or decrease 1 cm the working distance, respectively. Number 3 calibrates the working distance to the minimum distance. Finally, numbers 4 and 5 start and stop the axis movement, respectively.

Validation and characterization

Fiber production

The validation has been carried out by producing fibers with different polymers. Polystyrene (PS), poly (ethylene oxide) (PEO), and Polysulfone (PSF) were used to produce fibers with different processing conditions.

The protocol to prepare the polymer dissolutions was always the same. Polymer and solvent were mixed and stirred at least for 8 h until full dissolution (clear liquid). The proportion of solvents and polymer in the solutions used to prepare the materials are gathered in table 4.

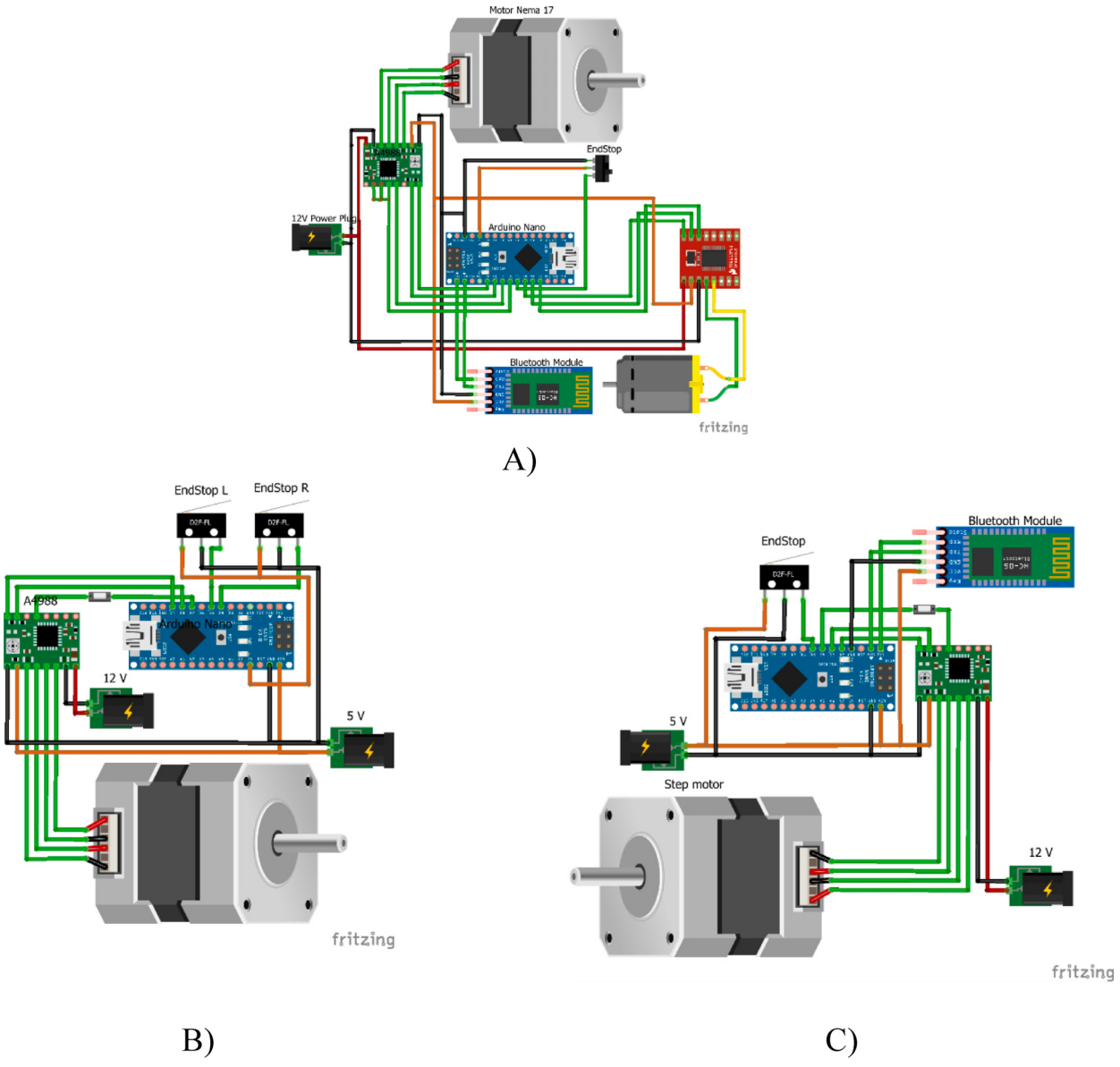

Fig. 10. Diagram of connections A) Syringe pump and collector, B) Movement of collector, and C) Work distance controller.

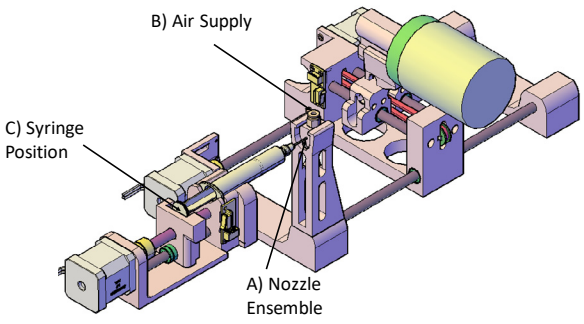

Fig. 11. Previous set up.

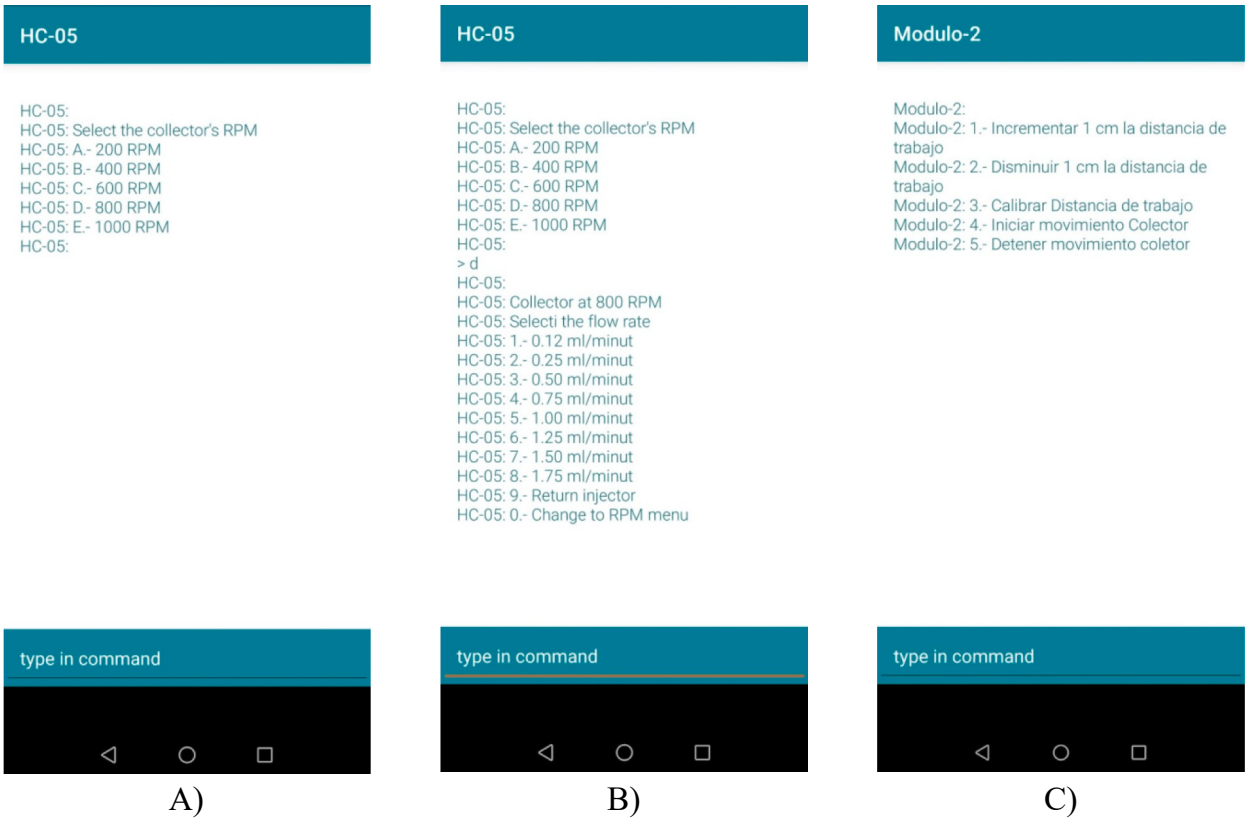

Fig. 12. Screens of Bluetooth controller of A) Speed of rotatory collector, B) Flow rate of syringe pump, and C) Working distance movement of collector.

Different conditions considered for each polymer dissolution were working distance (WD), air pressure (AP), and feed rate (FR) Table 5. In all the cases the polymer concentration in the dissolutions (10% w/v), protuberance of inner nozzle (2 mm), and inner nozzle diameter (0.6 mm), outer nozzle diameter (1 mm) was constant.

Morphology analysis was carried out using a Phillips XL30 Scanning electronic microscope (SEM) with an acceleration voltage of 10 kV, all samples were gold coated using a low vacuum coater Leica EM AC200 under 30 mA for 90 s.

Diameter of fibers (DoF) were evaluated by using free image analysis software ImageJ V.1.52a, US. Images were divided into four equal regions and then at least 20 independent and randomly chosen fibers were measured per region. Therefore, as least 80 measurements of fibers diameters were made to carry out statistical treatments. All statistical analysis was done with STATGRAPHICS Centurion XVI software (version 16.1.11).

Micro and Nano fibers were successfully spun using PEO, PS and PSF polymers separately. All the samples exhibit fibrous morphology as shown in Fig. 13. As can be seen, each polymer presents a specific morphology due to process parameters used for its production. PEO presents fibers without formations of beads (Fig. 13A), PS present fibrillary morphology with some beads (Fig. 13B), and PSF present a bead-on-string morphology (Fig. 13C). Although jet stability occurs with all the dissolutions to form fibers[16], PS and PSF showed formation of microconstituent.

In the case of PEO fibers, similar morphology was reported using an airbrush [29] and specialized nozzle [30]. Although Morphology of PEO fibers were similar, SBS parameter system used to produce them were different. In the case of airbrush, feed rate of polymer dissolution was by gravity, hence diameter of fiber could have varied [29]. Similarly, optimal concentration to produce fibers with PEO was reported [21] obtaining small diameters (278 nm) using a concentration of 6%, as consequence the use of 10% could be the cause of obtaining higher DoF as reported [31].

PS fibers with concentration of 10% (w/v) show the same morphology found when other technique as electrospinning is used [32,33]. Furthermore, similar morphologies were also reported with the SBS method [34]. Formation of beads could be

Table 4
Proportions of solvents and polymers used to prepare the materials.

Polymer	Weigh (g)	Solvent	Volume (ml)
PS	1	THF/Acetone	3/7
PEO	1	Chloroform/acetone	5/5
PSF	1	Chloroform/acetone	8/2

Table 5
SBS processing production of different polymers.

Polymer	WD (cm)	AP (bar)	FR (ml/min)	RPM collector
PEO	15	1.5	0.5	200
PS	15	1	0.75	200
PSF	25	1	0.25	200

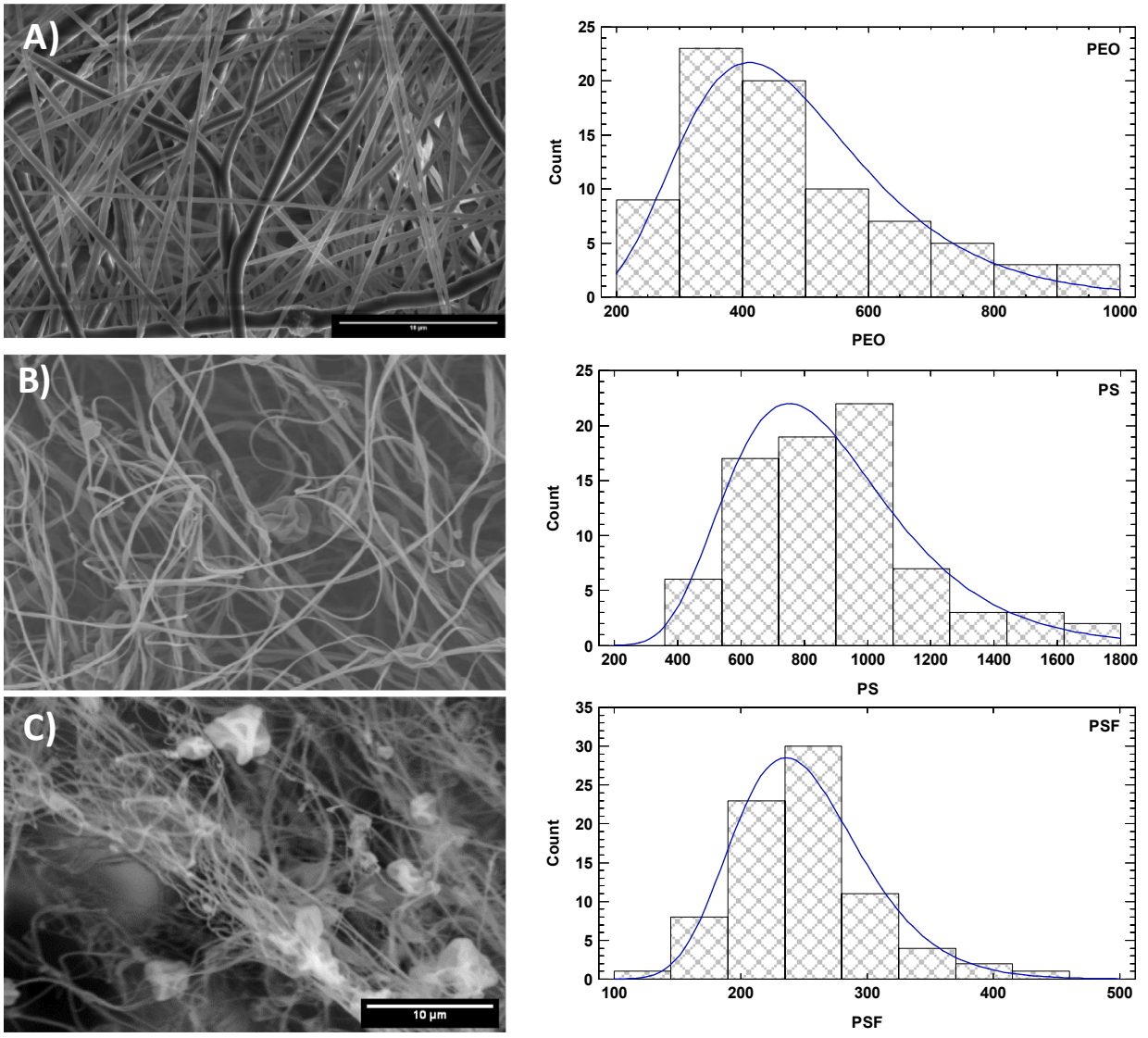

Fig. 13. SEM images and diameter distribution of PEO (A), PS (B), and PSF (C).

obtained with low concentrations because, in fact the concentration used was lower than the overlap concentration(C*). DoF was almost identical (table 6) as those reported with other SBS devices [35,36].

In the case of the polymer PSF it was reported the possibility of obtaining fibrous materials by SBS [20], however, bead-on-string morphology were not register yet by the use of this technique. Formation of fibers with beads seems to be mainly due to the concentration used. The number of molecular weight per unit volume characterized by the concentration of the dissolution and the length of the molecular chain can affect the viscosity of dissolution and hence the formation of bead-on-string fibers [37].

Each polymer system shows a specific fibrous morphology, so statistical analysis (Table 6) and ANOVA test were also conducted to study the differences between the materials morphologies.

Table 6
Statistical analysis of diameter of fibers.

Polymer	Experimental						Reference		
	Average (nm)	Median (nm)	SD (nm)	Error	Normality test (P-Value)	Lognormal test (P-value)	Average (nm)	SD (nm)	Ref
PEO	489	438	177	20	5.00E−08	≥0.10	642.9	474.8	[29]
PS	883	846	288	32	0.0129069	≥0.10	874	212	[36]
PSF	252	249	53	6	0.101213	≥0.10			

Diameter of fibers for each polymer was different due to the different nature of the polymers and differences in the processing conditions.

Anderson-Darling statistic (ADs) usually is a good way to identify different kinds of distributions. ADs was used to test the goodness of a certain distribution function used to fit the distribution of values associated to a sample population of size n. Hence, distribution of diameter values was tested by ADs for normal and lognormal fit. As a result, ADs indicates that PEO and PS cannot be well fitted by normal distribution (P-value $\leq$ 0.5). In the same way ADs test confirmed PEO, PS, and PSF experimental data can be well fitted by lognormal distribution (P-value $\geq$ 0.05) with a level of statistical significance of 95%.

Lognormal distribution is not a symmetric distribution therefore, study of average is no significant for treatment of data, so median DoF value (Fig. 14) was used to robust adjustment due this value is not affected by extreme.

One-way ANOVA test confirmed the different between fibers produced with the polymers (see the inserted table in Fig. 4) due to p-value (0.000 < 0.05) is shorter than significance level (95%) and F-value is sufficiently large, hence null hypothesis that diameter of fibers is similar was rejected.

Repeatability and reproducibility of fiber production

The repeatability and reproducibility of the process with this prototype were investigated. The repeatability is the capability to produce similar fibers to the previous one under the same processing conditions. The reproducibility is the capability to create a new batch of fibers with same characteristics using a reprinted nozzle.

Repeatability was confirmed by producing fibrous material with polymers as PSF, PS and PEO. Reproducibility was evaluated printing three nozzles by 3D printer and using them to produce fibers maintaining work distance (15 cm), Feed rate (0.5 ml/min), Air pressure (2 bars), polymer concentration (22%), inner nozzle (0.6 mm), outer nozzle (1 mm), protuberance (2 mm), speed of collector (200 RPM) and type of collector (Cylinder) constant. Then, one-way ANOVA was used to compare averages between samples.

Fig. 15 shows diameter of fibers produced by 3 different nozzles working under the same processing conditions. Diameter of fibers was in the range of 900 to 1500 nm. ANOVA analysis determinates there was no statistically significant difference between the means of the 3 variables with a level of 95.0% confidence due to P-value (0.0964) was highest than 0.05.

Influence of collector movement

System parameter as collector settings is not commonly registered but it has an important influence in the production of fibers by SBS. Although the top surface reflects the way the material is deposited on the substrate [38], it does not reflect the homogeneity of the material in terms of thickness along the collector.

Polysulfone material was used to know the influence of collector movement. The processing conditions used to produce the material were: work distance 15 cm, feed rate 0.5 ml/min, air pressure 2 bars and concentration 22%. Two sets were obtained, the first one was produced without movement of collector (Static) while the second one was obtained with constant speed movement of collector (Moving). For each set, six samples were collected directly in glass holders attached to

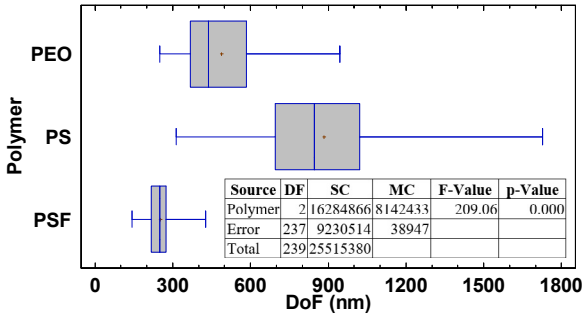

Fig. 14. One-way ANOVA test on DoF.

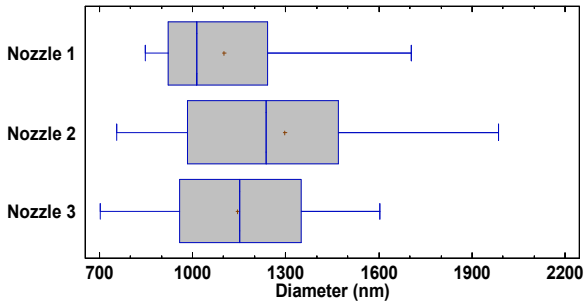

Fig. 15. Reproducibility of fibers.

Table 7
Average and standard deviation of thickness.

Zone	Static		Moving	
	Average (μm)	SD	Average(μm)	SD
1	161.0	99.7	514.0	32.7
2	234.0	90.7	534.0	39.2
3	441.0	66.9	554.2	56.6
4	701.5	87.7	608.2	36.2
5	934.2	98.6	651.0	36.5
6	1036.3	59.0	652.8	48.0
7	870.5	103.9	681.3	31.9
8	635.5	99.4	682.8	32.1
9	379.5	66.1	647.7	21.9
10	241.8	56.1	645.7	23.1
11	160.7	42.4	603.7	17.3

rotating cylinder and eleven zones along the glass holder were inspected to know the homogeneity in terms of thickness of the material deposited along the collector. Averaged results and standard deviations are shown in Table 7.

In electrospinning, fiber deposition could be controlled by ground position of voltage power supply, but in SBS method, deposition was not controlled by process parameter. In the case of SBS method, thickness of material was controlled by movement of collector, Visual Thickness of fibers collected on cylinder are shown in Fig. 16. Movement of collector creates and homogeneity layer with 616 μm ± 34 μm while static collector produces a layer in the shape of a mountain with a crest of 1036 μm ± 59 μm in the central part while in the most remote areas the thickness was 160 μm. It was caused the amount of fibers that are deposited at each zone of the collector as it moves.

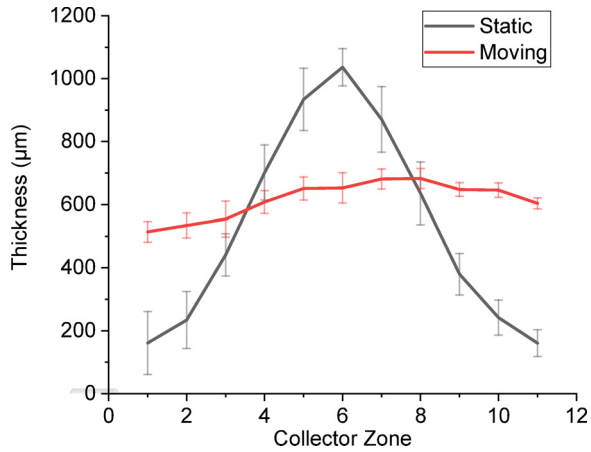

Fig. 16. Homogeneity of thickness.

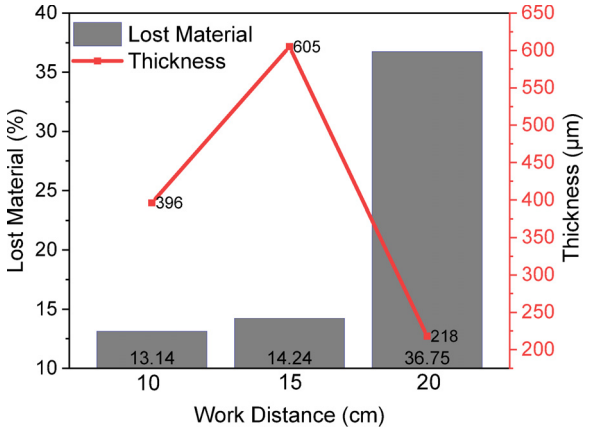

Fig. 17. Influence of working distance in quantity of material collected.

Influence of working distance

The influence of working distance in the diameter of fibers is not significant, however, the distance between the nozzle and collector influences the quality and quantity of the material collected. If the working distance is short, solvent evaporation does not occur efficiently and material in the form of film or constituted by welded fibers is collected. On the other hand, if the distance is too long, dry fibers might break during their time of flight to the collector, what could cause their dispersion and loss of material.

In order to evaluate the influence of working distance in term of quantity of material lost, the collector was weighed before and after producing the fibers for three different working distances used (10, 15 and 20 cm). Production parameters as feed rate (0.5 ml/min), air pressure (2 bars), PSF concentration (22%) protuberance (2 mm) were kept constant. The quantity of material lost, and the thickness of fibrous material obtained are shown in Fig. 17.

Although the working distance does not significantly influence the diameter of the fibers, the amount of material and the thickness of the material deposited can be greatly affected. As the WD increases, the quantity of fibers collected decreases and the thickness of the fibers also decreases.

In the case of PSF fibers, working distance of 10 and 15 cm does not significantly modify the amount of fibers obtained; however, the thickness of the material deposited changes. The WD distance parameter shows an open down parabolic tendency on the thickness of the deposited material on the collector. Probably short WD (10 cm) is used, the air pushes the fibers against the wall of the collector causing a decrease of thickness.

Declaration of Competing Interest

The authors declare that they have no known competing financial interests or personal relationships that could have appeared to influence the work reported in this paper.

Acknowledgements

Fondos de Investigación de Fco. Javier González Benito, política de reinversión de costes generales, Universidad Carlos III de Madrid [2012/00130/004] and Acción Estratégica en Materiales Compuestos Poliméricos e Interfases, Universidad Carlos III de Madrid [2011/00287/002]. Besides, authors greatly appreciate the Consejo Nacional de Ciencia y Tecnología (CONACyT-México) for financial support associated to the scholarship number 625396.

References

[1] R. Jones, P. Haufe, E. Sells, P. Iravani, V. Olliver, C. Palmer, A. Bowyer, RepRap – the replicating rapid prototyper, Robotica 29 (2011) 177–191, https://doi.org/10.1017/S026357471000069X.
[2] J.M. Pearce, N.C. Anzalone, C.L. Heldt, Open-Source Wax RepRap 3-D printer for rapid prototyping paper-based microfluidics, J. Lab. Autom. 21 (2016) 510–516, https://doi.org/10.1177/2211068215624408.
[3] B.T. Wittbrodt, A.G. Glover, J. Laureto, G.C. Anzalone, D. Oppliger, J.L. Irwin, J.M. Pearce, Life-cycle economic analysis of distributed manufacturing with open-source 3-D printers, Mechatronics 23 (2013) 713–726, https://doi.org/10.1016/j.mechatronics.2013.06.002.
[4] J.M. Pearce, Return on investment for open source scientific hardware development, Sci. Public Policy. 43 (2016) 192–195, https://doi.org/10.1093/scipol/scv034.
[5] K.C. Dhankani, J.M. Pearce, Open source laboratory sample rotator mixer and shaker, HardwareX 1 (2017) 1–12, https://doi.org/10.1016/j.ohx.2016.07.001.
[6] D. Trivedi, J. Pearce, Open Source 3-D printed nutating mixer, Appl. Sci. 7 (2017) 942, https://doi.org/10.3390/app7090942.

[7] B. Wijnen, E.J. Hunt, G.C. Anzalone, J.M. Pearce, G.F. Gilestro, Open-Source Syringe Pump Library, PLoS One 9 (2014) e107216, https://doi.org/10.1371/journal.pone.0107216.
[8] K. Pusch, T.J. Hinton, A.W. Feinberg, Large volume syringe pump extruder for desktop 3D printers, HardwareX 3 (2018) 49–61, https://doi.org/10.1016/j.ohx.2018.02.001.
[9] Y. Hiung, Y. Universiti, T. Hussein, C. Fhong, S. Universiti, T. Hussein, N.Z. Queen, Customizing a high flow rate syringe pump for injection of fluid to a microfluidic device based on polyimide film, ARPN J. Eng. Appl. Sci. 11 (2016) 3849–3855.
[10] C. Zhang, N.C. Anzalone, R.P. Faria, J.M. Pearce, Open-Source 3D-Printable Optics Equipment, PLoS One. 8 (2013) e59840. DOI:10.1371/journal.pone.0059840.
[11] T. Watson, N. Andrews, S. Davis, L. Bugeon, M.D. Dallman, J. McGinty, OPTiM: Optical projection tomography integrated microscope using open-source hardware and software, PLoS One. 12 (2017) e0180309. DOI:10.1371/journal.pone.0180309.
[12] B.J. Winters, D. Shepler, 3D printable optomechanical cage system with enclosure, HardwareX 3 (2018) 62–81, https://doi.org/10.1016/j.ohx.2017.12.001.
[13] J.Z. Milanovic, P. Milanovic, R. Kragic, M. Kostic, "Do-It-Yourself" reliable pH-stat device by using open-source software, inexpensive hardware and available laboratory equipment, PLoS One. 13 (2018) e0193744. DOI:10.1371/journal.pone.0193744.
[14] M.S. Islam, B.C. Ang, A. Andriyana, A.M. Afifi, A review on fabrication of nanofibers via electrospinning and their applications, SN Appl. Sci. 1 (2019), https://doi.org/10.1007/s42452-019-1288-4.
[15] S.K. Nune, K.S. Rama, V.R. Dirisala, M.Y. Chavali, Electrospinning of collagen nanofiber scaffolds for tissue repair and regeneration, Nanostructures Nov. Ther. Synth. Charact. Appl. (2017), https://doi.org/10.1016/B978-0-323-46142-9.00011-6.
[16] A. Chanthakulchan, P. Koomsap, K. Auyson, P. Supaphol, Development of an electrospinning-based rapid prototyping for scaffold fabrication, Rapid Prototyp. J. 21 (2015) 329–339, https://doi.org/10.1108/RPJ-11-2013-0119.
[17] Y. Gao, J. Zhang, Y. Su, H. Wang, X.-X. Wang, L.-P. Huang, M. Yu, S. Ramakrishna, Y.-Z. Long, Recent progress and challenges in solution blow spinning, Mater. Horizons. 8 (2021) 426–446, https://doi.org/10.1039/D0MH01096K.
[18] J.E. Domínguez, A. Kasiri, J. González-Benito, Wettability behavior of solution blow spun polysulfone by controlling morphology, J. Appl. Polym. Sci. 138 (2021) 50200, https://doi.org/10.1002/app.50200.
[19] V.E. Garcia, J. Liu, J.L. DeRisi, Low-cost touchscreen driven programmable dual syringe pump for life science applications, HardwareX. 4 (2018) e00027, https://doi.org/10.1016/j.ohx.2018.e00027.
[20] J. Teno, G. González-Gaitano, J. González-Benito, Nanofibrous polysulfone/TiO 2 nanocomposites: Surface properties and their relation with E. coli adhesion, J. Polym. Sci. Part B Polym. Phys. 55 (2017) 1575–1584, https://doi.org/10.1002/polb.24404.
[21] H. Lou, W. Li, C. Li, X. Wang, Systematic investigation on parameters of solution blown micro/nanofibers using response surface methodology based on box-Behnken design, J. Appl. Polym. Sci. 130 (2013) 1383–1391, https://doi.org/10.1002/app.39317.
[22] R.G.F. Costa, G.S. Brichi, C. Ribeiro, L.H.C. Mattoso, Nanocomposite fibers of poly(lactic acid)/titanium dioxide prepared by solution blow spinning, Polym. Bull. 73 (2016) 2973–2985, https://doi.org/10.1007/s00289-016-1635-1.
[23] G.H. Kim, Electrospinning process using field-controllable electrodes, J. Polym. Sci. Part B Polym. Phys. 44 (2006) 1426–1433, https://doi.org/10.1002/polb.20814.
[24] GeunHyung Kim, WanDoo Kim, Formation of oriented nanofibers using electrospinning, Appl. Phys. Lett. 88 (2006) 233101, https://doi.org/10.1063/1.2210972.
[25] J. Li, G. Song, J. Yu, Y. Wang, J. Zhu, Z. Hu, Preparation of solution blown polyamic acid nanofibers and their imidization into polyimide nanofiber mats, Nanomaterials 7 (2017) 395, https://doi.org/10.3390/nano7110395.
[26] D.D. da Silva Parize, M.M. Foschini, J.E. de Oliveira, A.P. Klamczynski, G.M. Glenn, J.M. Marconcini, L.H.C. Mattoso, Solution blow spinning: parameters optimization and effects on the properties of nanofibers from poly(lactic acid)/dimethyl carbonate solutions, J. Mater. Sci. 51 (2016) 4627–4638, https://doi.org/10.1007/s10853-016-9778-x.
[27] E.S. Medeiros, G.M. Glenn, A.P. Klamczynski, W.J. Orts, L.H.C. Mattoso, Solution blow spinning: a new method to produce micro- and nanofibers from polymer solutions, J. Appl. Polym. Sci. 113 (2009) 2322–2330, https://doi.org/10.1002/app.v113:410.1002/app.30275.
[28] G.C. Dias, T.S.P. Cellet, M.C. Santos, A.O. Sanches, L.F. Malmonge, PVDF nanofibers obtained by solution blow spinning with use of a commercial airbrush, J. Polym. Res. 26 (2019) 87, https://doi.org/10.1007/s10965-019-1731-7.
[29] J.G. Benito, J. Teno, D. Torres, M. Diaz, Solution Blow Spinning and Obtaining Submicrometric Fibers of Different Polymers, Int. J. Nanoparticles Nanotechnol. 3 (2017) 1–10. DOI:10.35840/2631-5084/5507.
[30] J.E. Oliveira, L.H.C. Mattoso, W.J. Orts, E.S. Medeiros, Structural and morphological characterization of micro and nanofibers produced by electrospinning and solution blow spinning: A comparative study, Adv. Mater. Sci. Eng. 2013 (2013) 1–14, https://doi.org/10.1155/2013/409572.
[31] J.E. Oliveira, E.A. Moraes, R.G.F. Costa, A.S. Afonso, L.H.C. Mattoso, W.J. Orts, E.S. Medeiros, Nano and submicrometric fibers of poly(D, L-lactide) obtained by solution blow spinning: Process and solution variables, J. Appl. Polym. Sci. 122 (2011) 3396–3405, https://doi.org/10.1002/app.34410.
[32] K.H. Lee, H.Y. Kim, H.J. Bang, Y.H. Jung, S.G. Lee, The change of bead morphology formed on electrospun polystyrene fibers, Polymer (Guildf). 44 (2003) 4029–4034, https://doi.org/10.1016/S0032-3861(03)00345-8.
[33] S. Huan, G. Liu, G. Han, W. Cheng, Z. Fu, Q. Wu, Q. Wang, Effect of experimental parameters on morphological, mechanical and hydrophobic properties of electrospun polystyrene fibers, Materials (Basel) 8 (2015) 2718–2734, https://doi.org/10.3390/ma8052718.
[34] A. Kasiri, J.E. Domínguez, J. González-Benito, Morphology optimization of solution blow spun polystyrene to obtain superhydrophobic materials with high ability of oil absorption, Polym. Test. 91 (2020) 106859, https://doi.org/10.1016/j.polymertesting.2020.106859.
[35] J.u. Lv, X. Yin, R. Li, J. Chen, Q. Lin, L.i. Zhu, Superhydrophobic PCL/PS composite nanofibrous membranes prepared through solution blow spinning with an airbrush for oil adsorption, Polym. Eng. Sci. 59 (2019) E171–E181, https://doi.org/10.1002/pen.v59.S110.1002/pen.24898.
[36] X. Zhang, J.u. Lv, X. Yin, Z. Li, Q. Lin, L.i. Zhu, Nanofibrous polystyrene membranes prepared through solution blow spinning with an airbrush and the facile application in oil recovery, Appl. Phys. A Mater. Sci. Process. 124 (5) (2018), https://doi.org/10.1007/s00339-018-1769-0.
[37] H. Zhao, H. Chi, Electrospun bead-on-string fibers: useless or something of value?, Nov Asp. Nanofibers (2018), https://doi.org/10.5772/intechopen.74661.
[38] J. González-Benito, J. Teno, G. González-Gaitano, S. Xu, M.Y. Chiang, PVDF/TiO2 nanocomposites prepared by solution blow spinning: surface properties and their relation with S. Mutans adhesion, Polym. Test. 58 (2017) 21–30, https://doi.org/10.1016/j.polymertesting.2016.12.005.

Professor José Ernesto Domínguez Herrera received his degree in Industrial engineering (specialist in manufacture) in 2007 by the technological institute of Orizaba (México). He received his master's degree in Learning science in 2010 by Institute of Higher Studies of State (México) afterwards, he received a masteŕs degree in Nanotechnology by Advanced Materials Research Center (México) in 2016. In 2021 he received his Ph.D. in Materials Science and Engineering from the Carlos III University of Madrid (UC3M). In 2012, he obtained a position as Associate Professor at Technological University of Veracruz (UTCV) in the industrial maintenance department and in 2018 as Professor in the Nanotechnology department. He researches activities focus on synthesis and characterization of nanofibers produced by the Solution Blow Spinning technique also design of prototypes with the open-source hardware philosophy. He is in the research group ''UTCV-CA-6 Technological Innovation for Sustainability" and collaborates with the research group ''Polymer Composites and Interphases" in the UC3M.